

Chapter 7

Summary and Implications

The aim of this thesis project was to better define the cross-scale evolution of heterogeneous deformation in BVT-segments of crustal-scale shear zones. Special emphasis was to be placed on the interaction in space and time of different deformation mechanisms during the formation of kilometer-scale shear zone networks in mechanically anisotropic rocks. In the first section of this chapter, the scientific results of the project will be summarized to link the individual chapters of this thesis. In a second section scientific implications of these results will be discussed.

7.1 Summary

7.1.1 Strain localization

Prior to the formation of the investigated shear zones at retrograde, greenschist facies metamorphic conditions psammitic and pelitic rocks, mainly composed of varying proportions of quartz, biotite, feldspar and muscovite, experienced a polyphase deformation during a high-temperature/low-pressure metamorphic evolution (Druguet, 2001). This study shows that the scales of millimeter- to 10m-scale shear zones correspond to the dimensions of mechanical anisotropies which formed during this metamorphic evolution (see below): A composite foliation with varying proportions of cleavage domains and microlithons on the millimeter-scale (Fig. 4.3), isoclinal folds of lithological layering on the centimeter- to decimeter-scale (Figs. 3.2 and 4.2) and layer-parallel pegmatites on the decimeter- to 10meter- scale (Fig. 6.7). All fabric elements are generally orientated at high angles to the bulk shearing

plane (Fig. 3.3).

Shear zone formation was shown to have involved a strain-dependent brittle-viscous transition, with fractures forming precursory to mylonitic shear zones. Fractures that are preserved in low-strain regions of the investigation area exhibit ductile damage zones¹ which are characterized by normal drags with sharp cut-offs towards the right-lateral fractures (Figs. 3.3, 3.4). Numerical models indicate that such drags cannot form due to frictional resistance during slip along *weak* faults (e.g. Reches & Eidelman, 1995, Grasmann et al., 2005). We interpret the normal drags to have resulted from the propagation of fractures through monoclinical folds that formed ahead of their tips ('ductile beads', Elliott, 1976). Ductile beads characterize terminations of both, investigated brittle fractures and mylonitic shear zones (Figs. 3.3, 3.4, 4.2, 7.1) which indicates that the processes described below represent the progressive structural evolution during strain localization (e.g. Mitra, 1984).

This evolution of shear zones was investigated by analyzing microstructures in samples from damage zones of fractures and mylonitic shear zones. This analysis revealed that progressive strain localization involved coeval fracturing, crystal-plastic deformation and a stress-induced reaction of biotite. The relative contributions of these processes to strain accommodation varied as a function of strain (Fig. 4.14).

Strain localization in tip damage zones commenced by elastic loading and work hardening, followed by brittle failure which dominated the early stages of strain localization. Fabrics in ductile beads were segmented by intragranular fractures. These interconnected with increasing strain to form transgranular microshears (Figs. 4.5 and 4.8). Fluid inclusion planes indicate the these processes might have been influenced by varying fluid pressures (Figs. 4.4). The strength of the rock in the tip damage zone is interpreted to have reached a maximum just prior to the formation of the transgranular microshears (Fig. 4.14a). Transgranular microshears contain a dynamically recrystallized polyphase fault rock which is interpreted to have formed from the host minerals by a combination of microcataclasis and pressure solution/precipitation (Fig. 4.12, Simpson, 1986, den Brock, 1992, van Daalen et al., 1999). Transgranular microshears are the microscale expression of decimeter-long shear fractures that characterize the damage zones of most

¹See Appendix 9.1 for terminology of shear zones and shear zone networks.

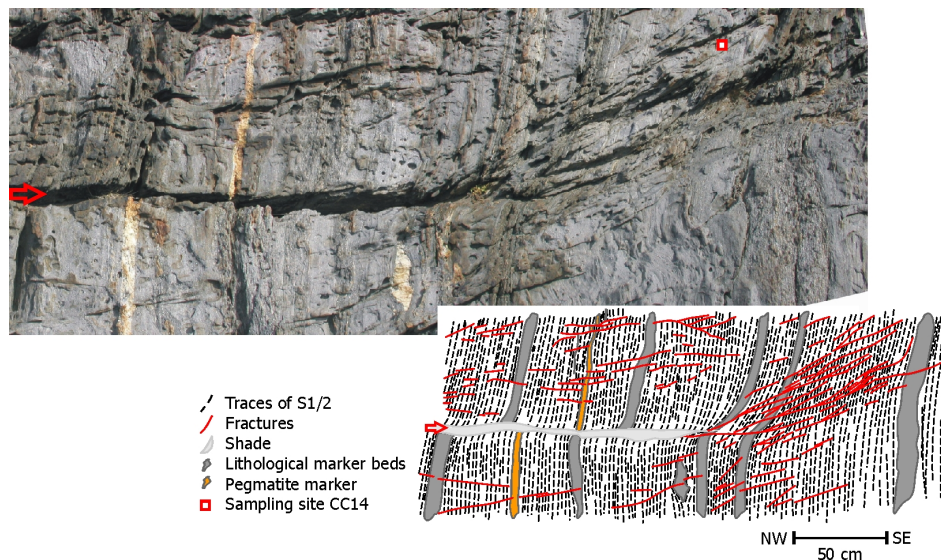


Figure 7.1: Several meter-long brittle shear fracture (F-shear zone) and its tip damage zone, which is characterized by a ductile bead and a splay of anticlockwise-deflected (with respect to the shearing plane) decimeter-long shear fractures. Line drawing by V. Georgieva. See text for explanation. Sampling site of sample CC14 (red square in photograph). Location UTM 31T 521859 east, 4687052 north.

shear zones in the investigated area (Fig. 7.1).

Fracture orientations were controlled by the composition of, and fabrics in the country rock (Fig. 4.10). High biotite contents and good alignment of biotite in cleavage domains oriented at high angles to the shearing plane caused antithetic deflections of propagating fracture tips (cf. Figs. 3.3, 4.10, 7.1, Gottschalk et al., 1990, Shea & Kronenberg, 1992, 1993). Deflected propagating fractures were responsible for the basic sigmoidal geometries that characterize the investigated shear zones networks (see below, Figs. 4.1, 5.14, Carreras, 2001).

Ductile beads are a macroscopic expression of mylonitic overprint of the rock in the tip damage zones of both, brittle and mylonitic shear zones. Dynamic recrystallization of quartz and a deformation-catalyzed reaction of biotite (Figs. 4.4c&d, 4.6, Kerrich et al., 1980, 1981) considerably weakened the country rock (White et al., 1980) and resulted in the formation of fine-grained aggregates (mainly) composed of quartz, biotite, muscovite, chlorite as well as ilmenite. After a critical displacement, the increasing volume proportion of the fine-grained mylonites was sufficient to govern the bulk

rheology of the rock in the tip damage zones and crystal plastic deformation and grain size sensitive creep replaced fracturing as the dominant deformation mechanism (Figs. 4.13, 4.14). This represents a strain-dependent brittle-viscous transition (BVT) which is responsible for the formation of mylonitic shear zone centers along shear fractures that exceed lengths of $\sim 10\text{-}15\text{m}$ and critical displacements of $\sim 120\text{-}150\text{cm}$. In tip damage zones of mylonitic shear zones, the BVT was attained after a bulk shear strain γ of ~ 1 . This numbers represent critical thresholds for the continued evolution of shear zones in space and time. Microstructures indicative of a strain-dependent brittle-viscous transition have been described from natural shear zones by, e.g., Segall & Simpson (1986) and van Daalen et al., (1999).

The evolution of the maximum shear strain (γ_{max}) in the shear zone center versus the average shear strain calculated over the entire shear zone width (γ_{mean}) with increasing displacement was shown to be indicative of the softening/hardening behavior of the shear zone. The two parameters (γ_{max} and γ_{mean}) are summarized in 'Iloc', the strain localization intensity, which describes the heterogeneity of strain distribution within a shear zone (Equation 6.5). A representative investigated shear zone exhibits a non-linear increase of (γ_{max}) with respect to (γ_{mean}) during progressive shearing (Table 3.1, Figs. 3.5, 6.10), which indicates significant softening in the shear zone center with time and strain (Type II of Hull, 1988, Means, 1995). This is supposed to have increased strain rates in the shear zone and thereby to have promoted its longitudinal propagation to lengths beyond the scale of the initial anisotropies (see above).

7.1.2 The formation of decameter-wide shear zones

The interaction of approaching parallel shear zones was influenced by the pre-existing foliation and lithological layering and controlled by antithetically deflected shear fractures propagating from their tips (Figs. 5.2a, 7.1). Furthermore, the interaction of neighboring shear zones may have been enhanced by the interplay of shear stress deviation fields which formed around their terminations and whose size is dependent on the viscosity contrast between the country rocks and the mylonite (Pollard & Segall, 1986, Lin & Logan, 1991, Nicholson and Pollard, 1985, Handy & Streit, 1999, Medvedev, 2006, pers. comm.). Both effects contributed to the formation of 'step-over' shear zones (sub-)parallel to the pre-existing foliation and sedimentary lay-

ering (at high angles to the bulk shearing plane), which interconnected 'host' shear zones (i.e., parallel to the bulk shearing plane) on adjacent shearing planes to form shear zone networks (Figs. 4.1, 5.14b). Lozenges of less-deformed country rock isolated in juvenile shear zone networks are about 15-30m long and exhibit length/width ratios of $\sim 2-3$, which may indicate some critical length scale for the interaction of shear stress deviation fields (Fig. 3.7).

Juvenile step-over shear zones are characterized by millimeter-wide, extremely fine-grained polyphase ultramylonitic layers (Figs. 5.3, 5.4, 5.6) that are interpreted to have formed by reactions of biotite and plagioclase (Figs. 5.9-5.11). These synkinematic reactions might have been enhanced by local stress-increases due to the rotation of isolated lozenges and step-over shear zones in bulk simple shear flow subsequent to shear zone networking (Fig. 5.14c&d). The ultramylonites exhibit a roughly homogeneous mineral phase distribution, lobate phase boundaries between biotite and quartz/feldspar, as well as transgranular sliding planes and lack evidence for intracrystalline deformation (Fig. 5.8). All of these observations combined evidence that deformation in the ultramylonites was dominated by diffusion-assisted solution/precipitation and viscous grain boundary sliding (e.g. Kerrich et al., 1980, Behrmann & Mainprice, 1987, Newman et al., 1999, Kruse & Stünitz, 1999). Thermometry done on synkinematic biotite and garnet from these shear zones indicates that the ultramylonites deformed at 400-500°C (Table 5.1, Fig. 5.12, Ferry & Spear, 1978, Hodges & Spear, 1982, Henry & Guidotti, 2002, Henry et al., 2005).

We consider step-over and host shear zones to have represented two independent slip systems during deformation of the shear zone network (cf. Mitra, 1979). A slip system is defined by the orientation of a shear zone and direction of movement along it (Gapais & Cobbold, 1987). The analysis of the shear zones constituting an investigated shear zone network indicate predominantly simple shear deformation (cf. Figs. 3.7, 3.8, Gapais & Cobbold, 1987, Gapais et al., 1987). Constant volume, compatible plane strain deformation in a shear zone network requires three independent slip systems (Mitra, 1979). The lack of a third independent slip system, the rotation of step-over shear zones in bulk simple shear flow as well as the tendency to minimize strain energy within the shear zone network are interpreted to have caused the lozenges to deform internally (cf. Hudleston, 1999, Figs.

3.10, 3.13). Rotation and widening reduced strain rates in step-over shear zones and the dominant deformation mechanism changed from dominantly viscous grain boundary sliding to a combination of grain size sensitive and crystal plastic deformation mechanisms in coarser grained mylonites. Ultramytonitic layers were preserved within the mylonites as step-over shear zones rotated synthetically towards the bulk shearing plane.

Lozenge deformation was achieved mainly by their compartmentalization and by widening of the adjacent shear zones (Figs. 3.10, 3.12). Widening of Type II (i.e. softening) shear zones (Hull, 1988, Means, 1995) was facilitated by fractures and vein-like ultramytonitic shear zones that truncated the country rock and segmented drags next to mylonitic shear zones (Fig. 5.2b). Drags segmented in this way experienced a pronounced mylonitic overprint (Fig. 3.11). Field evidence suggests that the fractures truncating drags propagated during shear zone activity (Fig. 3.11a).

Drag truncation (i.e. shear zone widening), lozenge compartmentalization and the rotation of step-over shear zones towards the bulk shearing plane resulted in the homogenization of strain distribution within the shear zone network (Figs. 3.12-3.14) and the formation of decameter-wide mylonitic shear zones that constitute the kilometer-scale Northern Shear belt (Fig. 3.1, Carreras, 2001). Deformation in these decameter-wide mature mylonitic shear zones was dominated by grain boundary bulging/subgrain rotation recrystallization in quartz (Stipp et al., 2002) and basal glide along [001] basal planes and pressure solution/precipitation in newly grown biotite. The rheology of these mylonites was governed by quartz and fine-grained aggregates of biotite, muscovite, ilmenite and chlorite, resulting from the stress-induced reaction of primary biotite (Figs. 4.6, 5.13). The differential stresses that drove this deformation were determined from 19,66 to 52,90MPa (Fig. 5.1, Koch, 1983), values that correspond well with paleopiezometric data from other midcrustal shear zones (e.g. Hacker et al., 1990, 1992, Gueydan et al., 2004).

7.1.3 Multiscaling of shear zones

The underlying geometry of the investigated shear zone networks is characterized by E-W trending step-over shear zones and NW-SE trending host shear zones from meter scales to the scale of the entire Northern Shear Belt (Fig. 3.1, Carreras 2001). To quantify the scaling relationships among

these shear zones we performed a multiscale analysis using Auto Correlation Functions to determine the areas of shear zones from two-dimensional image data. We investigated the evolution of the normalized shear zone area (LA, with respect to a representative reference area, RA) with shear zone length and width (LA/RA vs. length or width, Figs. 6.8, 6.9). Data clusters from shear zones on different length-scales were approximated by power-law functions whose exponents increase with shear zone length, from about 1 for centimeter-long shear zones to 2 for kilometer-long shear zones. We interpret, this change reflects that shear zone growth depends on strain- and scale-dependent parameters.

Interpreting the scaling analysis in the light of the time-sequence of shear zone development described above indicates that the scaling of centimeter- to meter-long shear zones is related to mechanical anisotropies in the host rock. Scales of shear fractures formed prior to mylonitic shear zones coincide with the dimensions of foliation spacing (millimeter- to centimeter scales, Figs. 4.8, 6.5), sedimentary layering (decimeter scales, Figs. 3.4, 4.2) and pegmatite bodies (meter- to decameter-scale, Figs. 6.7).

The continued growth of the shear zones was controlled by two factors (Fig. 6.12c): 1) The strain-dependent (i.e., related to a critical displacement) brittle-viscous transition of shear zones, which prevented the formation of shear fractures longer than about 10m and during which viscous creep became the dominant deformation mechanism, thereby weakening shear zone centers. 2) The interconnection of isolated shear zones to form shear zone networks, which depends on the interaction of propagating shear zones in parallel arrays. The interaction may have been influenced by the initial spacing of parallel shear zones and the viscosity contrast between mylonites and country rock. Within shear zone networks, strain energy is dissipated by lateral homogenization of strain instead of longitudinal growth of the network, which explains the nearly-quadratic power-law exponents. Networking of shear zone networks was associated with an upward-jump in the scale of the shear zones to decameter-wide shear zones some hundreds of meters to kilometers long. This "upscaling" (Handy et al., in press) contradicts conventional notions of strain localization in Type II shear zones, in which the deformation is considered to localize at smaller scales than the initial scale(s) of localization (e.g. Means, 1995).

7.2 Scientific implications

As outlined in the introduction (Chapter 2), deformation at the BVT is characterized by the coeval activity of brittle and viscous deformation mechanisms. Deformation at the BVT is supposed to be subject to substantial cyclic long-range variations in shear stress, strain rate and fluid pressures on the time-scale of the earthquake cycle (e.g. Handy et al., in press, and references therein). In the following, the questions whether such, seismically induced variations are preserved in the investigated shear zones and in which way they may influence the transitions between deformation mechanisms will be discussed.

- *Microstructures indicating coeval and/or subsequent brittle and viscous deformation do not show evidence for a cyclic reworking.* Microstructural analysis of rocks that were deformed along seismogenic faults in depth corresponding to the BVT show mutually overprinting cataclases, pseudotachylites and mylonites/ultramylonites (e.g. Passchier, 1982, 1984, Hobbs et al., 1986, Lin et al., 2005). Relevant microstructures indicative of multiple reworking and mutual overprinting of brittle and viscous deformation mechanism were not found in any of the investigated samples. However, transitions between brittle and viscous deformation mechanisms do occur, but they are restricted to the millimeter- to meter scale. Brittle fracturing is precursory to dislocation creep in shear zone propagation and widening and to grain-size sensitive creep in shear zone interconnection, respectively. Diffusion creep transiently dominates deformation in ultramylonitic shear zones but is replaced by dislocation creep as these shear zones widen. No indication for a brittle overprint of mylonites or ultramylonites was found. Therefore, transitions between deformation mechanisms at the Cap de Creus are generally one-way and clearly non-cyclic.
- *No major rupture plane(s) could be identified.* Theoretical predictions of crustal strength, rock structure and rheology during the earthquake cycle mostly describe the inferred distribution of these parameters upon the examples of single, crustal-scale shear zones (e.g. Sibson, 1986, Tse & Rice, 1986, Handy & Brun, 2004). Observations from natural earthquakes justify this simplification by showing that coseismic strains of large-magnitude earthquakes are usually accommodated

along a single or few, more or less interrelated fault planes (e.g. Wald & Heaton, 1994 for the 1992 Landers earthquake, Johanson et al., 2006 for the 2004 Parkfield earthquake). Aftershocks, that occur due to coseismic stress transfer are usually distributed over many more smaller faults in a much larger volume surrounding the coseismic slip patch (e.g. Beroza, 1991 for the 1989 Loma-Prieta earthquake, Liu et al., 2003 for the 1992 Landers earthquake).

Fossil examples of seismogenic fault planes usually exhibit a minimum dimension (e.g. Abercrombie, 1995). The rather *small dimension of the observed fractures limits the maximum seismic moments* that could have been reached during earthquakes. Fractures in our investigation area are between a few millimeters and $\sim 15\text{m}$ long. In most cases, displacements are not macroscopically detectable but they never exceed several decimeters. Cowan (1999) shows that very small seismic events (seismic moments $10^9 - 10^{12}\text{Nm}$) correspond to source dimensions of, expressed as radius of a circular source, about 10m and sub-millimetric slip increments. From these arguments we can not exclude the possibility that deformation along the observed fractures was seismic. However, we can exclude that the investigated shear zones formed major rupture planes that accommodated coseismic slip during large-magnitude earthquakes.

- Cowan (1999) argued that *faults are only recognizable as seismogenic in the field if pseudotachylites are preserved*. A few pseudotachylite layers were found in some of the investigation areas (Cala Portaló and Cala Cullaró, Fig. 3.1) but none of these could be identified as synmylonitic with respect to the investigated shear zone activity. Microstructural investigations (not shown in this thesis) indicate that the pseudotachylites were polyphase but did not experience a mylonitic deformation and I therefore assign them to a later, possibly Alpine deformation. No cataclasites were found in any of the investigated shear zones, with the exception of the submillimeter-wide fault rock in transgranular microshears, but these alone cannot be taken as proof for seismic events (Sibson, 1986).
- There is only *little evidence of unstable fracture propagation and sliding along existing faults*. The field and microstructural studies showed

that fractures formed at elevated temperatures and in the presence of small amounts of fluid, which indicates the possibility of extended periods of stable crack growth (Ghandi & Ashbi, 1979). Sliding along existent fracture planes was most probably assisted by extensive pressure solution/precipitation and followed by dynamic recrystallization after deactivation of the fractures, which points towards a stable sliding behavior.

Summarizing these arguments, it can be concluded that none of the observed structures is clearly indicative of earthquake activity. The fractures are suitably sized to have slipped unstably but as the microfabrics exclude the possibility of repeated mutual overprinting of brittle and viscous structures I conclude that the mylonitic shear zones at the Cap de Creus did not form first order rupture planes in relation with major earthquakes. Potential unstable slip along the investigated fractures may have occurred as a far field response to earthquakes in the overlying crust. However, the limited, millimeter- to meter scales at which transitions between brittle and viscous deformation mechanism occurred rather indicate that the scales of changes in boundary conditions promoting these transitions were limited, too.

Most transitions in deformation mechanisms are non-cyclic and 'one-way' and are therefore different from mutually overprinting brittle and viscous deformation related to the earthquake cycle (Sibson, 1980) or periodically occurring plastic instabilities producing temperature transients promoting melting (Hobbs et al., 1986, White, 1996). Brittle-viscous transitions are often related to shear zone propagation, where fracturing is supposed to promote an increased fluid flux, which enhances chemical softening and hydrolytic weakening (e.g. Segall & Simpson, 1986, Mancktelow & Pennacconi, 2005). Transitions from dislocation creep to grain-size sensitive creep are usually triggered by reaction softening during progressive deformation (e.g. Kerrich et al., 1980, Stünitz & Fitzgerald, 1993, Newman et al., 1999, Kenkmann & Dresen, 2002).

The field-, microstructural- and multiscaling analyses presented in this thesis clearly attribute transitions between deformation mechanisms to different stages in the progressive evolution of kilometer-scale shear zones. The specific changes in boundary conditions controlling these transitions were bound to these stages and therefore the transitions themselves were restricted to places where shear zones propagated, widened or interconnected.

Even though it is not possible to anticipate at which scale shear zone propagation, widening and strain homogenization (and thereby 'upscaling', Handy et al., in press) would have ended if deformation had continued, it is clear that the effects, that transitions in deformation mechanisms imposed on the deformation of crustal-scale faults, were limited to scales smaller than several tens of meters. The scientific results of this thesis therefore suggest that predictions of such transitions should always consider their extent and distribution in space.

